Nuclear Physics B322 (1989) 698–720
North-Holland, Amsterdam

BROKEN PHASE OF THE 4-DIMENSIONAL ISING MODEL IN A FINITE VOLUME

K. JANSEN[a,b], I. MONTVAY[c], G. MÜNSTER[d], T. TRAPPENBERG[a,b] and U. WOLFF[e]

[a] *Institut für Theoretische Physik E, Technische Hochschule Aachen, D-5100 Aachen, FRG*
[b] *HLRZ c/o KFA, P.O. Box 1913, D-5170 Jülich, FRG*
[c] *Deutsches Elektronen-Synchrotron DESY, Notkestraße 85, D-2000 Hamburg 52, FRG*
[d] *II. Institut für Theoretische Physik der Universität Hamburg, Luruper Chaussee 149, D-2000 Hamburg 50, FRG*
[e] *Institut für Theoretische Physik der Universität Kiel, D-2300 Kiel, FRG*

Received 29 November 1988

The volume dependence of physical quantities, like renormalized mass and coupling, is numerically investigated in the broken phase of the 4-dimensional Ising model. It is shown that finite volume effects in small and intermediate volumes are dominated by vacuum tunneling. The tunneling phenomenon is investigated in detail. The splitting of the ground states due to tunneling turns out to be given to a good approximation by an instanton-like calculation. The large volume limit of the physical quantities is compared to the prediction of the perturbative renormalization group which connects the scaling behaviour on both sides of the phase transition. A good agreement with the 3-loop β-function is observed.

1. Introduction

Quantum field theories with scalar fields and spontaneously broken symmetries play an important role in the standard model of elementary particle interactions, because they provide a theoretical framework for mass generation. In non-perturbative numerical simulations of these theories a detailed understanding of the finite volume effects is necessary, since numerical studies are always done in systems with finite volumes, but the interesting physical information is usually obtained in the infinite volume limit. A simple prototype quantum field theory with spontaneous symmetry breaking is the 4-dimensional Ising model which is equivalent to the single component ϕ^4 theory in the limit of an infinite bare quartic self-coupling.

In a series of previous papers [1–3] large scale numerical simulations of the 4-dimensional Ising model were performed by some of the present authors with special emphasis on finite volume effects. In ref. [1] the finite volume effects were studied in the symmetric phase and, in particular, numerical information on low energy scattering was extracted from the volume dependence of the 2-particle energy levels. In ref. [2] the scaling behaviour of the infinite volume renormalized

0550-3213/89/$03.50

coupling was investigated in the symmetric phase on large lattices by using an efficient cluster updating algorithm. In ref. [3] the vacuum tunneling phenomenon was studied and identified as the main source of finite volume effects in the broken phase. In the present paper, which is momentarily the last in this series, a detailed summary of the finite volume effects is given in the broken phase of the 4-dimensional Ising model and the large volume limit is compared to the scaling prediction obtained from previous results in the symmetric phase. The finite volume dependence of physical quantities is numerically studied and compared to analytic estimates. Tunneling on small and intermediate volumes is taken into account by an instanton-like calculation. On asymptotically large volumes, where tunneling is already negligible, the finite volume effects are calculated in renormalized perturbation theory. These analytical calculations will be described in sects. 2–4 of this paper and, as far as tunneling is concerned, also in ref. [4].

From the quantum field theory point of view the interesting region of bare parameter space is the vicinity of the critical point in both phases. In this region the cut-off is much larger than the physical scale, the cut-off dependence is very weak and to a good approximation the model can be considered as a continuum quantum field theory. A peculiarity of ϕ^4-theory is that in the scaling region the renormalized coupling is always small, in fact small enough for the applicability of renormalized perturbation theory. This can be seen, for instance, from the results of refs. [1, 2] and, more generally, from the approximate analytic solution of the 1-component ϕ^4 model [5, 6]. The renormalized coupling g_R as a function of the renormalized mass m_R is given by the Callan–Symanzik renormalization group equation [7]. For $m_R \to 0$, which means going to the critical point at $m_R = 0$, $g_R(m_R)$ tends to zero ("triviality" of ϕ^4). The asymptotic behaviours on the two sides of the critical point can be connected [6]. This allows to predict the renormalized coupling in the scaling region of the broken phase by starting the integration of the renormalization group equations from a point in the scaling region of the symmetric phase. Since g_R remains small, the perturbative β-function can be taken (this was the procedure used in ref. [6] for the analytic solution in the broken phase). Taking the precise numerical data of ref. [2] in the symmetric phase and the 3-loop perturbative β-function given in ref. [6] one can predict the expected renormalized coupling in the broken phase. However, as was noted in ref. [2], this extrapolation procedure is sensitive to the unknown higher corrections in the Callan–Symanzik β-function. An important aspect of the present calculation in the broken phase is to perform a direct numerical check of the 3-loop perturbative prediction.

The numerical simulations were performed both by the conventional local Metropolis algorithm and by the percolation cluster algorithm [8]. The latter was applied to study tunneling on lattices of size $10^3 \times 120$ as a function of the hopping parameter κ. In this case the percolation cluster algorithm is essential because of the possible global changes. On the large volumes, where tunneling is already negligible, and in our case the correlation length is between 2 and 3, it turned out to be

preferable to use the Metropolis algorithm. Details of the numerical calculations will be explained in sect. 5.

2. Basic definitions

In this section we consider the theory in an infinite volume. The 4-dimensional Ising model has variables $\phi_x = \pm 1$, which are associated with the points x of a hypercubical lattice $\mathbb{Z}^4$ in 4 dimensions. We use lattice units in this article which means that the lattice spacing a is set to 1. The action

$$S = -2\kappa \sum_x \sum_{\mu=1}^{4} \phi_x \phi_{x+\hat{\mu}}, \qquad \kappa > 0, \tag{1}$$

where $\hat{\mu}$ denotes the unit vector in the positive μ-direction, couples nearest neighbour points. This model is equivalent to a particular limit of the single-component ϕ^4 theory. The action of ϕ^4 theory on a lattice may be parametrized as

$$S = \sum_x \left(-2\kappa \sum_{\mu=1}^{4} \phi_x \phi_{x+\hat{\mu}} + \phi_x^2 + \lambda\left(\phi_x^2 - 1\right)^2 \right), \tag{2}$$

where the field ϕ assumes real values. In the limit of infinite bare quartic self-coupling $\lambda = \infty$ for fixed hopping parameter κ the Ising model is reproduced. Many of the definitions and considerations below also hold for finite values of λ. Expectation values of observables are defined in the usual way as averages with the Boltzmann factor $\exp(-S)$.

For values of κ above a certain critical κ_c the Z_2-symmetry $\phi \to -\phi$ of the action is broken spontaneously and the field acquires a non-zero vacuum expectation value:

$$\langle \phi_x \rangle = \pm v, \qquad v > 0. \tag{3}$$

This has to be taken into account in the calculation of connected expectation values like the propagator

$$G(x) = \langle \phi_x \phi_0 \rangle_c = \langle \phi_x \phi_0 \rangle - v^2. \tag{4}$$

The renormalized mass m_R and renormalized coupling g_R are defined in the same scheme as used in ref. [6]. The inverse propagator in momentum space yields m_R and the wave function renormalization Z_R through

$$\tilde{G}(p)^{-1} = 2\kappa Z_R^{-1}\left[m_R^2 + p^2 + O(p^4)\right]. \tag{5}$$

The physical particle mass m, which is different from m_R, is given by the pole of the

propagator closest to the origin:

$$\tilde{G}(p)^{-1} = 0, \qquad p = (im, 0, 0, 0). \tag{6}$$

In the scaling region m and m_R are nearly equal (see below).

The renormalized vacuum expectation value of the field is

$$v_R = \sqrt{2\kappa Z_R^{-1}}\, v, \tag{7}$$

and the renormalized coupling g_R is defined by

$$g_R = 3\,\frac{m_R^2}{v_R^2}. \tag{8}$$

This definition of course only makes sense in the phase with broken symmetry. The renormalized and the unrenormalized vertex functions are related through

$$\Gamma_R^{(n)}(p_1, \ldots, p_n) = \left(2\kappa Z_R^{-1}\right)^{-n/2} \Gamma^{(n)}(p_1, \ldots, p_n). \tag{9}$$

The renormalized 4-point vertex function defines another coupling

$$g_R^{(4)} = -\Gamma_R^{(4)}(0,0,0,0), \tag{10}$$

which equals g_R in tree-level perturbation theory (see below), but differs from it in higher orders. This quantity is normally used as a renormalized coupling in the symmetric phase, where v vanishes.

For the purpose of Monte Carlo calculations it is convenient to introduce the susceptibilities

$$\chi_n = \sum_{x_1, \ldots, x_{n-1}} \langle \phi_{x_1} \cdots \phi_{x_{n-1}} \phi_0 \rangle_c. \tag{11}$$

Since χ_2 is proportional to Z_R

$$Z_R = 2\kappa m_R^2 \chi_2, \tag{12}$$

the wave function renormalization cancels out in the ratios

$$\Lambda_n = \frac{\chi_n}{(\chi_2)^{n/2}}. \tag{13}$$

They are related to the vertex functions through

$$\Gamma_R^{(3)}(0,0,0) = m_R^3 \Lambda_3 ,$$

$$\Gamma_R^{(4)}(0,0,0,0) = m_R^4 \left(\Lambda_4 - 3\Lambda_3^2\right),$$

$$\Gamma_R^{(5)}(0,\ldots,0) = m_R^5 \left(\Lambda_5 - 10\Lambda_4\Lambda_3 + 15\Lambda_3^3\right),$$

$$\Gamma_R^{(6)}(0,\ldots,0) = m_R^6 \left(\Lambda_6 - 15\Lambda_5\Lambda_3 - 10\Lambda_4^2 + 105\Lambda_4\Lambda_3^2 - 105\Lambda_3^4\right),$$

$$\text{etc.} \tag{14}$$

The spectrum of states is conveniently described in the transfer matrix formalism. We denote the transfer matrix by e^{-H}, where H is the hamiltonian. In the symmetric phase ($\kappa < \kappa_c$) there is a unique ground state $|0_s\rangle$ which is symmetric with respect to the reflection $\phi \to -\phi$. Its energy E_{0s} is defined to be zero. The spectrum above this vacuum state corresponds to that of multi-particle states which are symmetric (s) or antisymmetric (a) under field reflection. The mass gap $m \equiv m_a$ is given by the energy E_{0a} of the antisymmetric one-particle state with zero momentum.

In the phase with broken symmetry ($\kappa > \kappa_c$) the ground state as well as all higher states are doubly degenerate. In the two vacua $|0_\pm\rangle$ the field has expectation values $+v$ and $-v$, respectively. They yield two sectors of the system such that matrix elements of local operators between different sectors vanish. The reflection $\phi \to -\phi$ transforms the sectors into each other. The spectra in both sectors are identical and again correspond to multi-particle states. The mass gap $m_+ = m_-$ is the single particle mass. As $\kappa \to \kappa_c$ the mass gap m_a (for $\kappa < \kappa_c$) or m_+ (for $\kappa > \kappa_c$) approaches zero.

3. The model in a finite volume

Numerical simulations of ϕ^4-theory or the Ising model are of course always done in a finite volume. The extrapolation to the infinite volume limit is associated with particular problems in the case of the broken phase. This situation will be discussed in the following. We consider a lattice with spatial volume L^3 and euclidean time extent T and periodic boundary conditions. With finite volume we mean finite L here, whereas T might also be considered infinite.

As is well known in statistical mechanics, spontaneous symmetry breaking does not occur in a finite volume. There is a unique symmetric ground state $|0_s\rangle$ as a consequence of the Frobenius–Perron theorem for the transfer matrix [9] and the vacuum expectation value of the field vanishes:

$$\langle 0_s | \phi_x | 0_s \rangle = 0 . \tag{15}$$

For $\kappa > \kappa_c$ transitions between the two sectors mentioned in the previous section occur and the degeneracy of states is lifted by tunneling. Above the ground state there is a lowest antisymmetric state $|0_a\rangle$ with a small energy $E_{0a} > 0$. If we write the ground state and the lowest antisymmetric state as

$$|0_s\rangle \equiv \frac{1}{\sqrt{2}} (|0_+\rangle + |0_-\rangle), \qquad |0_a\rangle \equiv \frac{1}{\sqrt{2}} (|0_+\rangle - |0_-\rangle), \tag{16}$$

then $|0_+\rangle$ and $|0_-\rangle$ are states which go over into the degenerate vacua in the infinite volume limit. Above these states we have the symmetric and antisymmetric one-particle states with momentum zero which are denoted by $|1_s\rangle$ and $|1_a\rangle$ and their energies by E_{1s} and E_{1a}, respectively.

The small energy splitting E_{0a} in the broken phase can be estimated in a semiclassical instanton-type calculation. In the one-loop approximation the result is

$$E_{0a} \simeq CL^{1/2} \exp(-\sigma L^3), \tag{17}$$

where a "surface tension" σ appears. More details on this are discussed in sect. 4.3.

The quantity

$$v \equiv \langle 0_s | \phi_x | 0_a \rangle \tag{18}$$

can be considered as a definition of the vacuum expectation value of the field in a finite volume. In the infinite volume limit it coincides with the usual definition

$$v = \langle 0_+ | \phi_x | 0_+ \rangle = -\langle 0_- | \phi_x | 0_- \rangle . \tag{19}$$

(For a discussion of possible finite volume definitions of the vacuum expectation value see refs. [10–13].) In a rigorous sense v cannot be determined through a measurement of the average field. This is manifest if one uses a global cluster updating algorithm in the Monte Carlo calculation as was the case in our work. In order to get v the propagator has to be analysed. For the calculation it is convenient to introduce the time slice averages

$$S_t \equiv \frac{1}{L^3} \sum_{\boldsymbol{x}} \phi_{\boldsymbol{x},t}, \qquad x = (\boldsymbol{x}, t). \tag{20}$$

Let

$$Z \equiv \mathrm{Tr}\, \mathrm{e}^{-TH} = 1 + \mathrm{e}^{-TE_{0a}} + \mathrm{e}^{-TE_{1s}} + \mathrm{e}^{-TE_{1a}} + \cdots \tag{21}$$

be the partition function. Then the vacuum expectation value of the product of time

slice field averages is given by

$$\begin{aligned}\langle S_0 S_t\rangle Z &\equiv \mathrm{Tr}\left(S_0 \mathrm{e}^{-tH} S_t \mathrm{e}^{-(T-t)H}\right)\\ &= v^2\left(\mathrm{e}^{-tE_{0a}} + \mathrm{e}^{-(T-t)E_{0a}}\right) + c_{01}^2\left(\mathrm{e}^{-tE_{1a}} + \mathrm{e}^{-(T-t)E_{1a}}\right)\\ &\quad + c_{10}^2\left(\mathrm{e}^{-tE_{0a}-(T-t)E_{1s}} + \mathrm{e}^{-(T-t)E_{0a}-tE_{1s}}\right)\\ &\quad + c_{11}^2\left(\mathrm{e}^{-tE_{1a}-(T-t)E_{1s}} + \mathrm{e}^{-(T-t)E_{1a}-tE_{1s}}\right) + \cdots ,\end{aligned} \tag{22}$$

where the matrix elements are defined as

$$c_{01} \equiv \langle 0_s|S_t|1_a\rangle , \qquad c_{10} \equiv \langle 1_s|S_t|0_a\rangle , \qquad c_{11} \equiv \langle 1_s|S_t|1_a\rangle . \tag{23}$$

If T and t are chosen suitably large the quantities v and E_{0a} can be extracted from the t-dependence of $\langle S_0 S_t\rangle$.

Based on eq. (22) one can also define the susceptibility χ_2 in the broken phase in a finite volume by subtracting from the summed 2-point function the contribution proportional to v^2:

$$\chi_2 \equiv \sum_x \langle \phi_0 \phi_x\rangle_c \equiv L^3 \sum_t \left(\langle S_0 S_t\rangle - v^2 \frac{\mathrm{e}^{-tE_{0a}} + \mathrm{e}^{-(T-t)E_{0a}}}{1 + \mathrm{e}^{-TE_{0a}}} \right) \tag{24}$$

for large enough T. This example demonstrates what kind of complications occur in Monte Carlo calculations in the broken phase due to the approximate degeneracy of states in a finite volume. It has to be taken into account in every correlation function. For the connected correlation of the time slice squared, which is also considered in our Monte Carlo calculation, one obtains for large volumes

$$\begin{aligned}\langle S_0^2 S_t^2\rangle_c &\equiv \langle S_0^2 S_t^2\rangle - \langle S_0^2\rangle^2\\ &= \Delta^2 \frac{\mathrm{e}^{-TE_{0a}}}{\left(1 + \mathrm{e}^{-TE_{0a}}\right)^2} + \frac{a_{01}^2}{1 + \mathrm{e}^{-TE_{0a}}} \mathrm{e}^{-tE_{1s}}\\ &\quad + b_{01}^2 \frac{\mathrm{e}^{-TE_{0a}}}{1 + \mathrm{e}^{-TE_{0a}}} \mathrm{e}^{-t(E_{1a}-E_{0a})} + \mathrm{O}\left(\mathrm{e}^{-TE_1}, \mathrm{e}^{-tE_2}\right),\end{aligned} \tag{25}$$

where we define

$$a_{01} = \langle 0_s|S_0^2|1_s\rangle , \qquad b_{01} = \langle 0_a|S_0^2|1_a\rangle \tag{26}$$

and the small quantity Δ is given by

$$\Delta = \langle 0_a|S_0^2|0_a\rangle - \langle 0_s|S_0^2|0_s\rangle . \tag{27}$$

For small t the second and third terms are relevant, whereas for large t only the first term survives.

4. Theoretical aspects

4.1. LATTICE PERTURBATION THEORY

For lattice ϕ^4-theory ordinary renormalized perturbation theory is applicable. The quantities of interest are expanded as power series in the renormalized coupling g_R, and the coefficients may depend on the renormalized mass m_R. In the case of physical quantities these coefficients have finite limits when the lattice spacing goes to zero. Near the critical point, where the renormalized coupling becomes small, it makes sense to consider renormalized perturbation theory whereas outside this region non-perturbative effects dominate.

The fact that g_R remains finite even in the Ising limit, where the bare quartic coupling λ goes to infinity, opens the possibility to use renormalized perturbation theory also for the Ising model. In this case the values of m_R for given values of g_R have to be specified as input coming from other sources beyond perturbation theory like Monte Carlo data or the hopping parameter expansion of Lüscher and Weisz [6].

In the broken phase perturbation theory is based on expanding the field around one of the minima of the (effective) action. The energy splitting and other tunneling phenomena are absent to all orders in perturbation theory. Therefore in perturbation theory the spectrum is doubly degenerate even in the case of a finite volume. In this subsection, however, we consider infinite volume perturbation theory.

A one-loop calculation yields the following expression for the inverse renormalized propagator:

$$-\Gamma_R^{(2)}(p) = m_R^2 + \hat{p}^2 + \tfrac{3}{2} g_R m_R^2 \left[J_2(m_R, \infty) + \hat{p}^2 I(m_R, \infty) - K(m_R, \infty, p) \right] + O(g_R^2), \tag{28}$$

where we define for arbitrary L

$$\hat{p}_\mu = 2 \sin \frac{p_\mu}{2},$$

$$J_n(m_R, L) = \frac{1}{L^3} \sum_k \int_{-\pi}^{\pi} \frac{dk_4}{(2\pi)} \left(\hat{k}^2 + m_R^2 \right)^{-n},$$

$$I(m_R, L) = -\frac{1}{3L^3} \sum_k \int_{-\pi}^{\pi} \frac{dk_4}{(2\pi)} \frac{\cos k_4}{\left(\hat{k}^2 + m_R^2 \right)^3},$$

$$K(m_R, L, p) = \frac{1}{L^3} \sum_k \int_{-\pi}^{\pi} \frac{dk_4}{(2\pi)} \left(\hat{k}^2 + m_R^2 \right)^{-1} \left(\widehat{(p-k)}^2 + m_R^2 \right)^{-1},$$

and the sums over $\boldsymbol{k}$ go over the Brillouin zone

$$k_i = \frac{2\pi}{L} n_i, \qquad n_i = 0,1,2,\ldots,L-1, \qquad i = 1,2,3. \tag{29}$$

For $L = \infty$ one obtains the following result for the physical mass m:

$$m = \overline{m} + \frac{3 g_{\mathrm{R}} m_{\mathrm{R}}}{4\sqrt{1+\frac{1}{4}m_{\mathrm{R}}^2}} \left[J_2(m_{\mathrm{R}},\infty) - m_{\mathrm{R}}^2 I(m_{\mathrm{R}},\infty) - K(m_{\mathrm{R}},\infty,q) \right] + \mathrm{O}\left(g_{\mathrm{R}}^2\right), \tag{30}$$

where

$$\overline{m} = 2\log\left(\tfrac{1}{2}m_{\mathrm{R}} + \sqrt{1+\tfrac{1}{4}m_{\mathrm{R}}^2}\right), \qquad q = (i\overline{m}, \mathbf{0}). \tag{31}$$

If $m_{\mathrm{R}} \leqslant 0.5$ ($g_{\mathrm{R}} \leqslant 31$) m deviates by less than 1.3% from m_{R}.

The one-loop expressions for the zero-momentum vertex functions are

$$\begin{aligned}
\Gamma_{\mathrm{R}}^{(3)}(0,0,0) &= -\sqrt{3g_{\mathrm{R}}}\, m_{\mathrm{R}}\left[1 + 3 g_{\mathrm{R}} m_{\mathrm{R}}^2 J_3 + \mathrm{O}\left(g_{\mathrm{R}}^2\right)\right], \\
\Gamma_{\mathrm{R}}^{(4)}(0,0,0,0) &= -g_{\mathrm{R}}\left[1 + 18 g_{\mathrm{R}} m_{\mathrm{R}}^2 J_3 - 27 g_{\mathrm{R}} m_{\mathrm{R}}^4 J_4 + \mathrm{O}\left(g_{\mathrm{R}}^2\right)\right], \\
\Gamma_{\mathrm{R}}^{(5)}(0,\ldots,0) &= -g_{\mathrm{R}}^2\sqrt{3g_{\mathrm{R}}}\, m_{\mathrm{R}}\left[15 J_3 - 90 m_{\mathrm{R}}^2 J_4 + 108 m_{\mathrm{R}}^4 J_5 + \mathrm{O}(g_{\mathrm{R}})\right], \\
\Gamma_{\mathrm{R}}^{(6)}(0,\ldots,0) &= -g_{\mathrm{R}}^3\left[15 J_3 - 405 m_{\mathrm{R}}^2 J_4 + 1620 m_{\mathrm{R}}^4 J_5 - 1620 m_{\mathrm{R}}^6 J_6 + \mathrm{O}(g_{\mathrm{R}})\right],
\end{aligned} \tag{32}$$

with $J_n \equiv J_n(m_{\mathrm{R}},\infty)$.

4.2. PERTURBATIVE FINITE VOLUME EFFECTS

The quantities considered in the previous section depend on L. In finite volume perturbation theory the lattice momenta flowing in loops are restricted to discrete values specified in eq. (29). For fixed values of the bare parameters κ and λ any renormalized quantity X deviates from the infinite volume limit by

$$\delta X(L) = X(L) - X(\infty). \tag{33}$$

This can be calculated in perturbation theory as power series in g_{R}. Renormalization conditions are imposed at $L = \infty$ which means that

$$g_{\mathrm{R}} \equiv g_{\mathrm{R}}(\infty), \qquad m_{\mathrm{R}} \equiv m_{\mathrm{R}}(\infty).$$

One-loop perturbative finite volume effects for some interesting cases are

$$\delta m_{\mathrm{R}} = -\frac{g_{\mathrm{R}}}{2m_{\mathrm{R}}}\left[\delta J_1 + \tfrac{3}{2}m_{\mathrm{R}}^2\,\delta J_2 - \tfrac{3}{2}m_{\mathrm{R}}^4\,\delta I + \mathrm{O}(g_{\mathrm{R}})\right],$$

$$\delta m = -\frac{g_{\mathrm{R}}}{2m_{\mathrm{R}}\sqrt{1+\tfrac{1}{4}m_{\mathrm{R}}^2}}\left[\delta J_1 + \tfrac{3}{2}m_{\mathrm{R}}^2\,\delta K(m_{\mathrm{R}}, L, q) + \mathrm{O}(g_{\mathrm{R}})\right],$$

$$\delta g_{\mathrm{R}} = -g_{\mathrm{R}}^2\left[\tfrac{3}{2}\delta J_2 - 3m_{\mathrm{R}}^2\,\delta I + \mathrm{O}(g_{\mathrm{R}})\right],$$

$$\delta v_{\mathrm{R}} = -\frac{\sqrt{3g_{\mathrm{R}}}}{2m_{\mathrm{R}}}\left[\delta J_1 + \tfrac{3}{2}m_{\mathrm{R}}^4\,\delta I + \mathrm{O}(g_{\mathrm{R}})\right],$$

$$\Delta Z_{\mathrm{R}} \equiv \frac{Z_{\mathrm{R}}(L)}{Z_{\mathrm{R}}(\infty)} - 1 = \tfrac{3}{2}g_{\mathrm{R}}m_{\mathrm{R}}^2\,\delta I + \mathrm{O}(g_{\mathrm{R}}^2), \tag{34}$$

where now

$$\delta J_n \equiv J_n(m_{\mathrm{R}}, L) - J_n(m_{\mathrm{R}}, \infty), \qquad \delta I \equiv I(m_{\mathrm{R}}, L) - I(m_{\mathrm{R}}, \infty).$$

These formulae can be used to extrapolate the Monte Carlo data to the infinite volume limit if tunneling effects are negligible and if the perturbative finite volume effects are sufficiently small.

4.3. TUNNELING

In intermediate volumes the finite size effects in the broken phase are dominated by tunneling. As discussed in sect. 3 the double degeneracy of states is lifted due to tunneling in a finite volume. In particular there is a vacuum energy splitting $E_{0\mathrm{a}}$, which can be calculated in a semiclassical approximation. In this section we consider the essential points of such a calculation and refer to ref. [4] for details.

The volume dependence of $E_{0\mathrm{a}}$ was studied in ref. [14], where the exponential factor in (17) was obtained from a Bloch wall picture. The prefactor $L^{1/2}$ was conjectured in ref. [15]. It differs from the usual WKB-factor $L^{3/2}$ coming from zero modes (see below) by an additional factor L^{-1} due to one-loop fluctuations.

We performed the calculation in the framework of the ϕ^4 theory. It is assumed that one is far enough in the scaling region such that finite lattice spacing effects are negligible and the calculation can be carried out in the continuum. The semiclassical calculation is based on an instanton-like saddle point approximation to the euclidean path integral as introduced in ref. [16] and beautifully explained in ref. [17].

To this end the tunneling amplitudes

$$\langle 0_+ | e^{-TH} | 0_\pm \rangle = \tfrac{1}{2}(e^{-TE_{0s}} \pm e^{-TE_{0a}}) \tag{35}$$

are expressed as path integrals with boundary conditions

$$\begin{aligned} \phi_x &\to v_0, \qquad T \to \infty, \\ &\to \pm v_0, \qquad T \to -\infty, \end{aligned} \tag{36}$$

where v_0 is the value of ϕ at the minimum of the classical action. In the case where $|0_-\rangle$ appears in eq. (35) the path integral is dominated by a classical solution, the so-called "kink":

$$\phi_c(x) = \sqrt{\frac{3m_0^2}{g_0}} \tanh \frac{m_0}{2}(x^4 - a) \tag{37}$$

with classical action

$$S_c = 2\frac{m_0^3}{g_0} L^3, \tag{38}$$

where m_0 and g_0 are the unrenormalized mass and coupling and a is a free parameter specifying the location of the kink. For fluctuations around the classical solution

$$\phi = \phi_c + \eta$$

the quadratic part of the action is given by

$$S = S_c + \tfrac{1}{2}\int d^4x\, \eta(x) M \eta(x) + O(\eta^3) \tag{39}$$

with the fluctuation operator

$$M = -\partial_\mu \partial^\mu + m_0^2 - \tfrac{3}{2}m_0^2 \cosh^{-2}\left[\tfrac{1}{2}m_0(x^4 - a)\right]. \tag{40}$$

The saddle-point approximation to the path integral amounts to integrating these gaussian fluctuations. The operator M has a zero-mode corresponding to translations of the kink or shifts of the parameter a. This zero-mode has to be treated separately by the method of collective coordinates. Taking into account also all contributions from non-interacting multi-kink configurations, which exponentiate,

the result for the energy splitting is

$$E_{0a} - E_{0s} = 2\,\mathrm{e}^{-S_c}\left(\frac{S_c}{2\pi}\right)^{1/2}\left|\frac{\det' M}{\det M_0}\right|^{-1/2}, \tag{41}$$

where det' is the determinant without zero-modes and

$$M_0 = -\partial_\mu \partial^\mu + m_0^2. \tag{42}$$

The factor $S_c^{1/2} \sim L^{3/2}$ is due to the zero-mode. The determinant, which represents a one-loop effect, leads to the following three types of contributions. First of all it produces precisely those counterterms which are required to convert the unrenormalized parameters appearing in eq. (41) into the renormalized ones. Moreover, it yields an additional factor L^{-1}. Finally it gives a one-loop correction to the term proportional to L^3 in the exponential. The final result is of the form (17) with

$$C = 1.65058\sqrt{2\frac{m_R^3}{g_R}} \tag{43}$$

and an L-dependent surface tension

$$\sigma(L) = \sigma_\infty\left(1 - \frac{g_R}{16\pi^2}\,\frac{3\sqrt{3}\,\pi}{(m_R L)^2}\exp\left(-\tfrac{1}{2}\sqrt{3}\,m_R L\right) + \mathrm{O}(\mathrm{e}^{-m_R L}) + \mathrm{O}(g_R^2)\right), \tag{44}$$

$$\sigma_\infty = 2\,\frac{m_R^3}{g_R}\left[1 - \frac{g_R}{16\pi^2}\left(\frac{1}{8} + \frac{\pi}{4\sqrt{3}}\right) + \mathrm{O}(g_R^2)\right]. \tag{45}$$

A comparison of these one-loop formulae with the results of the Monte Carlo calculation is made in section 5.3.

5. Monte Carlo calculation

5.1. CLUSTER ALGORITHM

To obtain the numerical results presented in this paper we employed both the standard local Metropolis algorithm and the new global cluster updating scheme of Swendsen and Wang (SW) [8]. The former was found to be superior due to its suitability for vectorization when the volume in the broken phase is large enough to make vacuum tunneling effects irrelevant. Use of the SW-algorithm on the other hand was advantageous in the symmetric phase [2] and crucial to investigate tunneling in the broken phase which there turned out to be the dominant finite size

effect [3]. We now briefly describe the SW-algorithm in the Ising model as we used it in our simulation.

We consider the Ising model on a d-dimensional hypercubic lattice Λ with partition function

$$Z = \sum_{\phi_x = \pm 1} e^{-S}, \tag{46}$$

where S is the action (1). The SW-algorithm can be derived easily if we introduce additional redundant bond variables $k_{x\mu} = 0, 1$:

$$Z = A^{|\Lambda| d} \sum_{\phi_x = \pm 1,\, k_{x\mu} = 0,1} e^{\alpha \Sigma_{x\mu} k_{x\mu}} \Delta(k|\phi). \tag{47}$$

Here $\Delta(k|\phi)$ expresses the constraint that bonds with $k_{x\mu} = 1$ can only exist between parallel spins:

$$\Delta(k|\phi) = \prod_{x\mu} \left[1 + \tfrac{1}{2} k_{x\mu} (\phi_x \phi_{x+\mu} - 1)\right]. \tag{48}$$

The partial summation over $\{k_{x\mu}\}$ in eq. (47) can easily be carried out and if we match

$$\alpha = \log(e^{4\kappa} - 1), \qquad A = e^{-2\kappa} \tag{49}$$

equivalence with eq. (46) is achieved in the sense that all correlations of spins ϕ_x coincide. In principle we may also perform the partial $\{\phi_x\}$ summation in eq. (47) and get

$$Z = A^{|\Lambda| d} \sum_{k_{x\mu}} e^{\alpha \Sigma_{x\mu} k_{x\mu}} 2^{\nu[k_{x\mu}]}, \tag{50}$$

where $\nu[k_{x\mu}]$ is the number of disconnected clusters when $k_{x\mu} = 1$ (0) is interpreted as active (passive) bond in the sense of bond percolation. There is a factor 2 for each cluster in eq. (50) from its independent spin orientations, and this is a special case of the Fortuin–Kasteleyn [18] representation of Potts models. In the SW-algorithm one performs Monte Carlo sampling for both $\{k_{x\mu}\}$ and $\{\phi_x\}$ in alternating order. Clearly, for fixed $\{\phi_x\}$ the $\{k_{x\mu}\}$ distribution factorizes and an independent new choice $\{k_{x\mu}\}$ has to be done. For fixed $\{k_{x\mu}\}$ a spin direction has to be assigned randomly to each cluster as a whole. The non-trivial step consists of decomposing the lattice sites into clusters. We used the algorithm described in ref. [2] and also the more standard Hoshen–Kopelman [19] method. The latter could be tuned to execute 30% faster in the case of the cluster structure in the 4-dimensional Ising model at the κ values we investigated. Either method of cluster search is recursive and could not be vectorized in contrast to all other routines we used. It is intuitively

clear that the SW-algorithm has the power to reduce critical slowing down. We may regard $\{k_{x\mu}\}$ only as a vehicle to get from one spin configuration to the next which then differs from the old one by large domains of flipped spins. These are precisely the moves which are needed to explore vacuum tunneling [3] and which are produced very slowly via local updates.

The cluster structure accessible from updating can be exploited further for variance reduction. An arbitrary spin observable $O(\phi_x)$ may be replaced by a bond dependent $\tilde{O}(k_{x\mu})$ with the same mean by the formula

$$\tilde{O}(k_{x\mu}) = 2^{-\nu[k_{x\mu}]} \sum_{\{\phi_x = \pm 1\}} \Delta(k|\phi) O(\phi_x). \tag{51}$$

The improved observable $\tilde{O}(k_{x\mu})$ takes into account all conceivable spin assignments of the clusters even if only one of them is used as the next configuration. For instance, improved observables for odd powers of the spin vanish identically and thus give the right answer for finite volume with zero variance. The improved counterpart of the two-point function is the cluster incidence function

$$\langle \phi_x \phi_y \rangle = \langle \Theta(x, y) \rangle, \tag{52}$$

where $\Theta(x, y)$ is 1 if x, y are in the same cluster and 0 otherwise. As discussed in more detail in ref. [20] the respective variances V are

$$V[\phi_x \phi_y] = 1 - \langle \phi_x \phi_y \rangle^2 \tag{53}$$

versus

$$V[\Theta(x, y)] = \langle \phi_x \phi_y \rangle (1 - \langle \phi_x \phi_y \rangle). \tag{54}$$

We see that the variance reduction becomes most profitable when the physical interest focuses on correlations decaying to small values as e.g. in the symmetric phase of ϕ^4 theory [2]. In this paper we shall also have occasion to use the improved four-point function

$$\langle \phi_{x_1} \phi_{x_2} \phi_{x_3} \phi_{x_4} \rangle = \langle \Theta(x_1, x_2)\Theta(x_3, x_4) + \Theta(x_1, x_3)\Theta(x_2, x_4) + \Theta(x_1, x_4)\Theta(x_2, x_3) - 2\Theta(x_1, x_2, x_3, x_4) \rangle, \tag{55}$$

where the four-point incidence function $\Theta(x_1, x_2, x_3, x_4)$ is the obvious generalization of the two-point one $\Theta(x_1, x_2)$. When correlations are summed to give susceptibilities or zero momentum couplings, simple expressions in terms of the numbers of spins in the various clusters result.

In general, the error estimates for simple directly measured observables were performed by observing quadratic fluctuations and correcting for correlations between successive measurements. This is achieved sometimes by measuring the time autocorrelations and mostly by blocking the measurements until they become independent to a good approximation. Where compared, both methods gave consistent errors.

For more intricate quantities like connected correlations and minimal χ^2-fit parameters we proceeded as follows. We successively divided our large number of measurements into $1, 2, 4, \ldots, 128$ subsamples. In each subsample the direct observables are averaged (blocked) and fits and appropriate combinations are then made. The fluctuations of the latter among the subsamples of equal size are used to estimate errors which become stable for a sufficient number of subsamples. Always the best mean value is used from fits and combinations in the full sample.

5.2. NUMERICAL SIMULATIONS

We started our numerical simulations in the same way as in the previous work in the symmetric phase [1]. In short runs an appropriate κ-value was searched for, where the mass in lattice units is about $\simeq 0.5$. This turned out to be $\kappa = 0.077$. In this point a series of high statistics runs was performed by the Metropolis algorithm on $L^3 \times T$ lattices. We took $T = 16$ which is somewhat larger than in a similar point in the symmetric phase ($T = 12$) [1], because on the basis of the Lüscher–Weisz solution [6] and using the perturbative estimates in sect. 4 we expected somewhat stronger finite size effects in the broken phase. In these runs the vacuum expectation value of the field v was simply defined by the absolute value of the average spin over the lattice. This definition is the usual one in finite volume numerical simulations. It was investigated in detail in the Ising model by Binder [12] and it is expected to converge for large volumes to the correct infinite volume vacuum expectation value. Taking the absolute value is essential, because in the finite volume the expectation value of the average spin is always zero if sufficiently long runs are performed. In the broken phase this means that the system tunnels between the two minima of the effective potential. The question how long the run has to be depends on the simulation algorithm. For the local Metropolis algorithm on larger lattices the flips of the average spin sign are rather rare (see below), but with the global cluster algorithm described above a few sweeps suffice. Having defined the vacuum expectation value in such a way, other expectation values with odd field parity can also by defined by imagining that the spin configuration was multiplied by -1 if the average spin is negative. This method of defining expectation values with odd field parity in the broken phase can be shortly referred to as the "reflection method".

Even before knowing the results of the $L^3 \times 16$ simulations we felt somewhat uneasy about the reflection method. It is clear that, especially if the average field is

TABLE 1
The results of the numerical calculation on $L^3 \times 16$ lattices at $\kappa = 0.077$. 10 million sweeps per lattice were done with every fifth measured. Error estimates in last numerals are in parentheses. The expectation values are defined here by the reflection method.

L	m	v	χ_2	$-\Lambda_3$	$\Lambda_4 \times 10^{-3}$	$-\Lambda_5 \times 10^{-6}$	$3\Lambda_3^2 - \Lambda_4$
6	0.277(2)	0.35033(19)	40.35(12)	68.3(2)	4.93(4)	−0.12(1)	9050(30)
8	0.505(3)	0.38485(6)	21.81(7)	83.2(9)	21.6(6)	8.5(3)	−850(130)
10	0.545(2)	0.38871(3)	18.75(3)	53.1(5)	7.8(3)	2.1(2)	670(160)
12	0.553(3)	0.38931(3)	18.31(2)	48.7(4)	6.0(2)	1.2(1)	1130(120)
14	0.553(2)	0.38945(2)	18.24(2)	47.8(4)	5.4(2)	1.1(1)	1420(180)
16	0.554(1)	0.38947(2)	18.18(2)	47.8(6)	5.5(3)	2.4(2)	1390(220)

near zero, this procedure is quite arbitrary. In any case it introduces additional finite size effects which are rather difficult to estimate analytically. Our reservations were strengthened by the results of the $L^3 \times 16$ runs (see table 1).

Table 1 shows that the finite volume effects are very strong on small lattices (up to 10^3). Especially the quantities like Λ_n involving a high degree of cancellation seem to be very sensitive. In fact, they show an erratic behaviour on small lattices. (For instance, the negative sign in the last column at $L = 8$ is not a misprint!) At $\kappa = 0.076$ similar confusing results appeared on lattices up to $L = 12^3$. A possible attitude is to disregard the small lattices on the basis of "too strong finite size effects", but in this case the theoretical control over the finite volume effects is essentially given up.

It is intuitively clear that strong finite volume effects on small lattices may be due to the vacuum tunneling discussed in sect. 3. Therefore we decided to investigate tunneling in detail. This is best done on lattices which are very long in the time direction because then the small splitting of doubled energy levels can be determined. The use of the cluster algorithm described in the previous subsection makes it possible to sample the tunneling configurations in an effective way. The results of the runs on lattices $L^3 \times 120$ were described in detail in ref. [3], where the κ- and volume-dependence of the low-lying spectrum was investigated with $L = 8$, and at $\kappa = 0.076$, respectively. The expected behaviour of the low-lying zero momentum spectrum could be verified, showing, for instance, that the analytic continuation of the symmetric one-particle state in the broken phase is the lowest two-particle state in the symmetric phase. At $\kappa = 0.077$ on the 8^3 lattice tunneling is still important. Although the splitting of the antisymmetric and symmetric vacua is already small ($E_{0a} \simeq 0.006$, see table 1 of ref. [3]), the one-particle mass is still ill-defined because the symmetric and antisymmetric one-particle states have rather different energies: $E_{1s} \simeq 0.4$ and $E_{1a} \simeq 0.5$. This explains why the more subtle quantities with a structure specific to the broken phase (like Λ_n) are completely distorted.

TABLE 2
The results of the numerical calculation on $10^3 \times 120$ lattices. The number of sweeps is given in thousands (ks). Error estimates in last numerals are in parentheses. v and χ_2 are defined here by the invariant method described in sect. 3.

κ	ks	E_{0a}	E_{1s}	E_{1a}	v	χ_2
0.0740	251	0.2292(6)	0.516(2)		0.1185(2)	
0.0745	243	0.1700(6)	0.419(2)		0.1366(4)	
0.0750	244	0.1044(5)	0.328(3)		0.1688(6)	
0.0755	300	0.0424(2)	0.275(5)	0.47(6)	0.2265(4)	8(3)
0.0760	361	0.00902(6)	0.329(8)	0.366(8)	0.2958(2)	35.0(6)
0.0765	247	0.00114(6)	0.462(5)	0.464(7)	0.34810(15)	26.8(5)
0.0770	222	0.0001(1)	0.543(4)	0.545(3)	0.38890(9)	18.6(3)

In order to see the evolution of tunneling as a function of volume for different hopping parameters, we also performed a series of simulations with the cluster algorithm on a $10^3 \times 120$ lattice. The vacuum expectation value (v) and susceptibility (χ_2) were determined by the formulas in sect. 3. This procedure can be called the "invariant method" because only invariant quantities with respect to the field reflection $\phi_x \to -\phi_x$ are used. The results are collected in table 2. For an example of the behaviour of the correlation functions see ref. [21]. A graphical comparison of the spectrum with the $8^3 \times 120$ data from ref. [3] is shown in fig. 1.

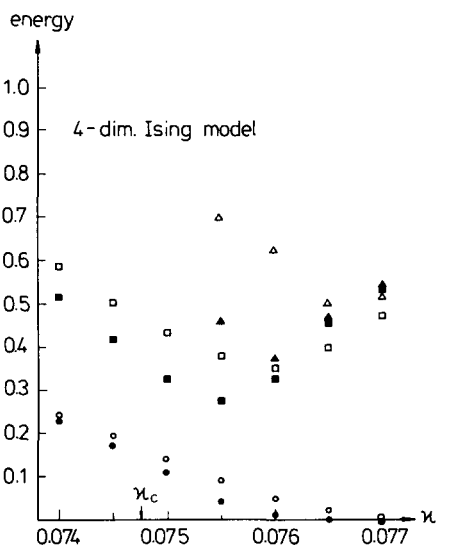

Fig. 1. The hopping parameter dependence of the low-lying momentum spectrum on $8^3 \times 120$ lattice (open symbols) and $10^3 \times 120$ lattice (full symbols). The energy levels, as defined in sect. 3, are circles for E_{0a}, squares for E_{1s} and triangles for E_{1a}.

TABLE 3
Comparison of the predictions of renormalized perturbation theory for finite volume effects in large volumes with numerical data obtained from table 1. For each L the first line shows the perturbative results. The second line is obtained from the results of the numerical simulation. It takes into account the correction factor m_R/m, which is taken from perturbation theory and is near 1.016 for all L. The errors are calculated from those of table 1 by the usual law of error propagation. The input parameters m_R and g_R for perturbation theory are chosen such that $m_R(L)$ and $g_R(L)$ match the Monte Carlo data for $L = 16$. The perturbative prediction for the finite L-correction $\Delta Z_R(L)$ is always smaller than the error of Z_R and therefore not displayed.

L	m_R	m	g_R	$-\Lambda_3$	$\Lambda_4 \times 10^{-3}$	$g_R^{(4)}$	Z_R
10	0.558	0.549	35.4	47.8	5.4	79	
	0.554(2)	0.545(2)	35.1(5)	53.1(5)	7.8(3)	63(15)	0.886(6)
12	0.561	0.553	35.8	47.0	5.2	83	
	0.562(3)	0.553(3)	36.1(7)	48.7(4)	6.0(2)	113(12)	0.890(9)
14	0.562	0.554	36.0	46.7	5.1	85	
	0.562(2)	0.553(2)	35.9(5)	47.8(4)	5.4(2)	141(18)	0.886(6)
16	0.563	0.554	36.0	46.6	5.1	86	
	0.563(1)	0.554(1)	36.0(2)	47.8(6)	5.5(3)	139(22)	0.886(3)
∞	0.563	0.554	36.1	46.6	5.1	86	

Comparing v and χ_2 in tables 1 and 2 one can see that at $\kappa = 0.077$ on the 10^3 lattice the reflection method and the invariant method give very similar results which differ by less than the statistical errors. Similarly, the mass m obtained by the reflection method is also equal to E_{1s} and E_{1a} within small errors. This means that for these quantities tunneling is negligible. It is possible, however, that for other quantities as e.g. Λ_n the effect of tunneling is still important and one has to go to larger volumes in order to suppress it. In this respect one has to note that tunneling can occur not only globally for the whole lattice, but also for some parts of it, and the quantities involving a large degree of cancellation may be more sensitive to these partial tunnelings.

Once vacuum tunneling is negligible, for the estimate of the finite volume effects one can apply renormalized perturbation theory, which is an expansion around one of the vacua. Taking m, v and χ_2 for $L = 16$ from table 1 as input data, one can determine m_R, Z_R and g_R by using the formulas given in sect. 4. From the renormalized mass and coupling at infinite volume the volume dependence of every renormalized physical quantity can be determined. The one-loop formulas given in sect. 4 are compared with the numerical results in table 3.

For $L \geqslant 10$ the agreement of the data with renormalized perturbation theory can be considered satisfactory, especially for the largest lattices, but in this case the deviations from the infinite volume are already small and comparable with the statistical errors. In this respect the situation becomes worse at $\kappa = 0.076$ where, as

TABLE 4
The results of the numerical calculation on L^4 lattices at $\kappa = 0.076$. The number of sweeps is given in millions (Ms). The quantities were measured after every fifth Metropolis sweeps. Error estimates in last numerals are in parentheses.

L	Ms	E_{1s}	E_{1a}	v	χ_2	Z_R	g_R	$g_R^{(4)}$
16	10	0.386(2)	0.389(2)	0.30130(3)	38.35(6)	0.895(8)	29.8(5)	38(12)
20	7.5	0.3914(12)	0.3909(14)	0.30158(2)	37.85(6)	0.893(4)	30.2(4)	92(24)

noted before, tunneling effects are still strong on a 12^3 lattice. At the same time, the perturbative finite size effects on 14^3 are already very weak, actually smaller than our statistical errors. In other words, the measurable finite volume effects are dominated by tunneling. At this κ value the numerical results on our largest lattices are collected in table 4.

5.3. VACUUM SPLITTING AND INSTANTONS

As described in subsect. 4.3 and in more detail in ref. [4], the energy splitting of the vacuum state can be estimated by a one-loop instanton calculation. Here we compare the prediction, eqs. (43)–(45) with the Monte Carlo data. At $\kappa = 0.076$ the values of the surface tension σ and the constant C in (17) have been determined from a fit of E_{0a} up to $L = 10$ in ref. [3], namely

$$\sigma = 0.00358(2), \qquad C = 0.101. \tag{56}$$

With the value $m_R = 0.395(1)$ obtained from table 5 we get the dimensionless ratio

$$\sigma/m_R^3 = 0.0581(5). \tag{57}$$

On the other hand the theoretical prediction with $g_R = 30.2(4)$ is

$$\sigma_\infty/m_R^3 = 0.0589(8), \qquad C = 0.105(1). \tag{58}$$

Including also the L-dependence in eq. (44) yields a small correction:

$$\sigma/m_R^3 = 0.0585(8) \qquad \text{for } L = 10. \tag{59}$$

The agreement with the numbers above is remarkably good.

TABLE 5
Comparison of the results of the numerical simulation from tables 3 and 4 with the predictions of ref. [6]. The numbers to the right of LW are obtained from table 3 in ref. [6].

	κ	m_R	g_R	Z_R
MC	0.077	0.563(1)	36.1(2)	0.886(3)
LW	0.0767(4)	0.56	35(4)	0.920(15)
MC	0.076	0.395(1)	30.2(4)	0.893(4)
LW	0.0759(2)	0.40	27(2)	0.929(14)

The small energy difference E_{0a} gives also the tunneling rate for a local updating algorithm, as for instance the Metropolis algorithm [15,22]. The average number of sweeps between two consecutive sign flips of the average spin is approximately

$$\tau_L \sim \frac{1}{E_{0a}^2} \sim L^{-1} \exp(2\sigma L^3) . \tag{60}$$

In order to obtain τ_L we have performed MC runs, using the Metropolis algorithm, on 8^4, 10^4 and 12^4 lattices at $\kappa = 0.076$ and monitored the tunneling events. This was done by calculating v averaged over different blocks of measurements, where the number of measurements in a block is 2^n, $n = 1, \ldots, 16$. If for a given block size v changes its sign on successive blocks, we stored this as one "flip event".

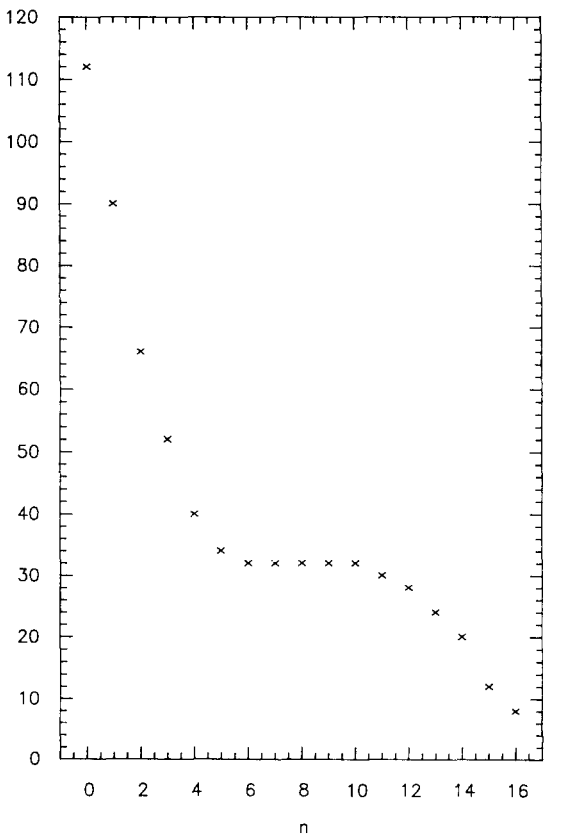

Fig. 2. The number of flip events on the 12^4 lattice at $\kappa = 0.076$ as function of the block length 2^n. The run has 1 Msweeps in total.

If now the block length is too small one overestimates the flip rate, as every fluctuation of the system is registered as a flip event. If the block length is too large one clearly underestimates the flip rate as one integrates over a number of flip events. So one expects to observe a plateau in the number of flip events if it is plotted as a function of the block length. Indeed, fig. 2 shows such a behaviour for a 12^4 lattice. Similar pictures are obtained for the other lattices. Extracting τ_L for a given lattice size from the plateau, one can fit the L-dependence according to eq. (60). The result of the fit is

$$\sigma = 0.00289(7)\,. \tag{61}$$

This is in qualitative agreement with the value in eq. (56).

5.4. CHECK OF THE SCALING CONNECTION

The infinite volume renormalized mass and coupling extracted from our numerical simulation data can be compared to the Lüscher–Weisz solution [5, 6].

In most cases the agreement is good within the indicated errors. Somewhat larger deviations are, however, observed for Z_R. The errors of the numerical calculation are smaller than the errors estimated in ref. [6].

The analytical solution in the broken phase is based on the connection between the scaling behaviours on the two sides of the critical point. This connection can be considered as a consequence of the relation between initial data at vanishing renormalized mass ($m_R = 0$) for the solutions of the renormalization group equations at either side of the critical point. In order to exploit this connection one has to integrate the renormalization group equations starting from a finite renormalized mass and determine the asymptotic behaviour for $m_R \to 0$. Since the natural variable is $\log m_R$, it is a long way to go from any finite m_R to $m_R = 0$, and therefore the unknown higher loop corrections to the Callan–Symanzik functions may influence the asymptotics considerably. In order to check the scaling connection on the two sides of the critical point we can take the last measured point in the symmetric phase from ref. [2] at $m_R = 0.3078(3)$ and start the integration of the renormalization group equations there. Using the 3-loop functions together with the 1-loop lattice artifact corrections as given in refs. [5, 6] we obtain at $m_R = 0.395$ in the broken phase the prediction

$$g_R[m_R = 0.395] = 30.6 \pm 1.1\,, \qquad Z_R[m_R = 0.395] = 0.918 \pm 0.009\,. \tag{62}$$

The errors indicated here correspond to the uncertainty of the initial data. g_R is in excellent agreement with table 4. For Z_R there is, however, a small discrepancy. Using the two-loop functions would not change the prediction for Z_R essentially, but the renormalized coupling would be changed to $g_R(m_R = 0.395) \simeq 35.7$. Therefore, the three-loop prediction agrees clearly better with the numerical data. The

situation concerning the convergence of renormalized perturbation theory looks good from this point of view. Nevertheless, one has to note that in our points at $\kappa = 0.077$ and 0.076 the renormalized coupling is not very small. In some quantities, as for instance $g_R^{(4)}$, the convergence of the perturbation series is quite poor. For $\kappa = 0.076$ (where the coupling is smaller), the one-loop result with $g_R = 30.2$ is $g_R^{(4)} \simeq 62$ [note that at tree level $g_R^{(4)} = g_R$ and the numerical value in table 4 is $g_R^{(4)} = 92(24)$]. Therefore, a real stringent test of the perturbative scaling connection can only be performed at smaller masses.

6. Conclusion

With the present paper we conclude our detailed numerical study of the 4-dimensional Ising model. In these investigations [1–3] our main emphasis was put on the aspects important from the point of view of particle physics, namely the determination of physical masses and couplings in the infinite volume limit. The precision achieved is in general satisfactory. Generally speaking, the fortunate circumstance in this simple 4-dimensional quantum field theory model is the fact that besides the precise numerical simulations also analytical tools are available and the combination of these two methods is possible.

Concerning the broken phase studied in the present paper, an important conclusion is that the finite volume effects on small and intermediate volumes are dominated by vacuum tunneling. In order to have full control over the tunneling effects, we investigated the behaviour of the system on lattices elongated in the time direction (see also ref. [3]). In particular, the low-lying zero momentum energy spectrum was determined as a function of volume and hopping parameter. The splitting of the states reflecting the existence of two vacua could be measured. The behaviour of the energy of the antisymmetric ground state was compared to an instanton calculation [4] and very good agreement was found. This energy vanishes exponentially with the volume, and therefore it gives a very large correlation length which can be measured on elongated lattices. This phenomenon is expected to be characteristic of first order phase transitions, where there are two (or more) degenerate ground states. (Note that in the Ising model there is a first order phase transition at $\kappa > \kappa_c$ as a function of the external magnetic field.) It is not impossible that the large correlation length observed by the Ape Collaboration [23] at the deconfining phase transition in pure gauge QCD is due to this vacuum tunneling phenomenon.

The renormalized mass and coupling was extrapolated to infinite volume from large lattices where the effect of tunneling is negligible. This extrapolation can, in principle, be controlled by using the estimates of the asymptotic finite volume effects given by renormalized perturbation theory. In practice the perturbative corrections turned out to be small, in most cases comparable to the statistical errors on large lattices.

The values obtained for the renormalized mass and coupling agree with the predictions of Lüscher and Weisz [6] which are based on the scaling connection on the two sides of the critical point. Taking the results of the simulations at $\kappa = 0.0732$ in the symmetric phase [2] and at $\kappa = 0.076$ in the broken phase the scaling connection can directly be checked. A very good agreement with the 3-loop perturbative renormalization group functions is found, although in the vicinity of the points measured in the broken phase the convergence of renormalized perturbation theory for some quantities is quite poor.

We thank Jiri Jersák for helpful discussions. This work is supported by Deutsches Bundesministerium für Forschung und Technologie and the Deutsche Forschungsgemeinschaft. The Monte Carlo calculations have been performed on the CRAY X-MP/48 of HLRZ, Jülich and on the CRAY X-MP/18 of the University of Kiel and we thank these institutions for generous grants of computer time.

References

[1] I. Montvay and P. Weisz, Phys. B290 [FS20] (1987) 327
[2] I. Montvay, G. Münster and U. Wolff, Nucl. Phys. B305 [FS23] (1988) 143
[3] K. Jansen, J. Jersák, I. Montvay, G. Münster, T. Trappenberg and U. Wolff, Phys. Lett. B213 (1988) 203
[4] G. Münster, Nucl. Phys. B, to be published
[5] M. Lüscher and P. Weisz, Nucl. Phys. B290 [FS20] (1987) 25
[6] M. Lüscher and P. Weisz, Nucl. Phys. B295 [FS21] (1988) 65
[7] E. Brézin, J.C. Le Guillou and J. Zinn-Justin, *in* Phase transitions and critical phenomena, eds. C. Domb and M.S. Green (Academic Press, London, 1976) Vol. 6, p. 125
[8] R.H. Swendsen and J.-S. Wang, Phys. Rev. Lett. 58 (1987) 86
[9] C. Domb, Adv. Phys. 9 (1960) 149
[10] C.N. Yang, Phys. Rev. 85 (1952) 808
[11] T.D. Schultz, D.C. Mattis and E.H. Lieb, Rev. Mod. Phys. 36 (1964) 856
[12] K. Binder, Z. Phys. B43 (1981) 119
[13] R. Griffiths, Phys. Rev. 152 (1966) 240
[14] M.E. Fisher, J. Phys. Soc. Japan Suppl. 26 (1969) 87;
V. Privman and M.E. Fisher, J. Stat. Phys. 33 (1983) 385
[15] E. Brézin and J. Zinn-Justin, Nucl. Phys. B257 [FS14] (1985) 867
[16] A.M. Polyakov, Nucl. Phys. B120 (1977) 429
[17] S. Coleman, *in* The whys of subnuclear physics, Erice lectures (1977), ed. A. Zichichi, (Plenum, New York, 1979), *reprinted in* S. Coleman, Aspects of Symmetry (Cambridge University Press, Cambridge, 1985)
[18] P.W. Kasteleyn and C.M. Fortuin, J. Phys. Soc. Japan Suppl. 26 (1969) 11;
C.M. Fortuin and P.W. Kasteleyn, Physica 57 (1972) 536
[19] J. Hoshen and R. Kopelman, Phys. Rev. B14 (1976) 3438
[20] U. Wolff, Nucl. Phys. B300 [FS22] (1988) 501
[21] K. Jansen, *in* Proc. Fermilab Conf. on Lattice field theory (September 1988), to be published
[22] J.C. Niel and J. Zinn-Justin, Nucl. Phys. B280 [FS18] (1987) 355
[23] Ape Collab., P. Bacilieri et al., Phys. Rev. Lett. 61 (1988) 1545